INVESTIGATION OF AN UNUSUALLY SHALLOW EARTHQUAKE SEQUENCE IN MOGUL, NV FROM A DISCRIMINATION PERSPECTIVE

Ileana M. Tibuleac, Glenn Biasi, David von Seggern, John G. Anderson, and Danielle Molisee

University of Nevada, Reno

Sponsored by the Air Force Research Laboratory

Award No. FA9453-11-1-0236
Proposal No. BAA11-51

ABSTRACT

Distinction between very shallow (1-4 km deep) earthquakes and underground nuclear explosions remains an important issue in discrimination research. This is because very shallow earthquakes are seldom well-recorded and documented. As a consequence, their source parameters, scaling and their local and regional propagation characteristics are not well understood. Thus, unlike for deeper events, the effectiveness of the discrimination algorithms when applied to unusually shallow earthquakes has been only rarely determined. The primary objective of this study is a detailed investigation of a sequence of earthquakes that occurred during 2008 west of Reno, Nevada, in Mogul. This sequence consisted of over 1700 earthquakes with M_L of 1.0 or greater, concentrated in depth between 1 and 4 km and ranging in magnitude up to M_w 5.0 (the "main shock"). Preliminary analyses of the main shock have revealed uncharacteristically high amplitude near-field ground motions and uncharacteristically rapid attenuation with distance, which could affect the magnitude estimates and the discrimination metrics. For our investigations, we use a unique broadband and strong-motion recording database, from stations as close as 1 km from the epicenter of the main shock and most of the smaller events. We have organized our study in four tasks: First, our investigations started by building a detailed shallow event database. In addition to available public domain information on very shallow event discrimination analysis, the database includes near-field and seismic network recordings of all the M_L>1.0 Mogul, Nevada earthquakes located by the Nevada Seismological Laboratory; mining explosions (M_L>2.0) and crustal earthquakes (M_L>2.5) in the in the Reno-Carson City, NV, area; the waveforms from the 1993 Rock Valley sequence (depth < 4 km, m_b≤4.3) and waveforms from the 2007 Crandall Canyon mine collapse, (M_L 3.9). The objectives of the second task are to analyze the stress drop and radiated energy of the main shock, principal foreshocks, and principal aftershocks as well as to investigate the source scaling of the Mogul sequence. We will estimate source parameters (moment, corner frequency, stress drop) for $M_L \geq 3.5$ Mogul events using three related methods: 1) Spectral measurements; 2) Empirical Green's Functions and 3) Measurements of *Lg/Sn* coda envelopes. Third, we will investigate the effect of source depth on *P* and *S* spectra and spectral ratios, signal complexity, and the m_b versus M_s discriminant. Fourth, we will attempt to understand the origin and nature of the near-source attenuation and its effect on magnitude estimates and energy content-related discriminant performance. We will compare our results to other very shallow earthquake sequences, induced seismicity and nuclear explosions results.

OBJECTIVES

The objective of our study is to investigate the effectiveness of discrimination algorithms when applied to an unusually shallow (1-4 km deep) sequence of well-documented earthquakes, which occurred 2008 in western Nevada. In addition, we are investigating source parameters, scaling and local and regional propagation characteristics of these earthquakes in comparison to other relevant shallow events.

RESEARCH ACCOMPLISHED

An important aspect of nuclear explosion monitoring is event identification. Because earthquakes less than 4 km deep are rare, and their characteristics are poorly known, it is difficult to rule them out as suspect events. The earthquake sequence that occurred in 2008 west of Reno, Nevada, beneath the community of Mogul (Figure 1) was unusual for several reasons relevant to nuclear monitoring. First, events in this swarm were exceptionally shallow, with the bulk of the seismic activity taking place at depths of 1-4 km (Figure 2). Only few other sequences occurring above the 5 km deep upper limit of the "seismogenic zone" were observed in California (Fletcher et al., 1987; Frankel et al., 1986, Prejean and Ellsworth, 2001) and Nevada (Smith et al., 2006). Second, the protracted run-up provided time to instrument the epicentral area with temporary broadband and strong-motion stations, in advance of the largest events. These stations complimented the Nevada and California permanent seismic monitoring stations, and the high-quality broadband stations of the Earthscope Transportable Array network deployed in Nevada in 2008. Third, the main shock (M_w 5.0) had exceptional (Figures 3 and 4) source and attenuation characteristics (Anderson et al., 2009). The Mogul sequence included 11 events with local magnitude 3.5 or greater, had swarm-like behavior and accelerating moment release leading up to the main shock.

The methods to distinguish between very shallow crustal earthquakes and underground nuclear explosions are not well developed, significantly because such well-instrumented, very shallow earthquakes are so rare. We plan to apply recognized discrimination algorithms to the larger earthquakes of the Mogul swarm and to compare the results to corresponding studies of explosions and to more typical crustal earthquakes. We seek to answer the question whether events from the unusually shallow Mogul earthquake sequence could have been positively identified as earthquakes using the tools available to the monitoring community.

We are currently within the first phase of a research program in which our investigations began by building a detailed shallow event database. In addition to available public domain information on very shallow event discrimination analysis, the database includes:

1) All the M_L>1.0 shallow earthquakes located by the Nevada Seismological Laboratory (NSL) in Mogul, NV and the set of near-field recordings. Regional and teleseismic records of the largest Mogul events are currently collected from Incorporated Research Institutions for Seismology (IRIS) and the Air Force Research Laboratory. This database (Figure 1) also includes earthquakes in the Mogul sequence located at more than 4 km depth. Nine earthquakes in the 2008 Mogul sequence (M_L> 2.5) have been located at the Nevada Seismological Laboratory (NSL) at depths from 4 to 7 km.

The Mogul earthquakes increased in frequency and magnitude over a period of two months starting in February 2008, in a pattern consistent with accelerating moment release (Figure 2). Four M_L>3.0 events occurred on April 15, 2008, followed by two M_L > 4 events on April 24th, and the main shock on April 25th (23:40 local time, 4/26/2008 06:40 GMT; M_L 4.7; M_w 5.0). Ultimately the swarm produced over 3500 events of M_L> 0.6, of which eleven had magnitude $M_L \geq 3.5$. The swarm occurred at the edge of the Reno, NV permanent strong-motion network operated by the NSL in cooperation with the United States Geological Survey (USGS) Advanced National Seismic System (ANSS). The regional seismic network in western Nevada and eastern California, the Southern and Northern California Seismic Networks, and the Earthscope Transportable Array broadband network recorded the larger Mogul events to distances of several hundred kilometers. As the swarm escalated, the NSL installed a ten-station portable seismograph array in west Reno (~4 km aperture). The portable seismographs, provided by the IRIS Rapid Array Mobilization Program (RAMP), were configured with collocated broadband sensors and force-balance accelerometers, recording at least 100 sps. Four were installed in the epicentral area by April 9th, in time to record the largest foreshocks and the main shock (Figure 4). Six additional temporary stations were installed in the epicentral area in early May 2008, and they recorded until early August 2008. Of the 38 $M_L \geq 3.0$ earthquakes in the Mogul sequence, 32 were recorded with at least four stations in the epicentral area and one or more stations within one kilometer of the epicenter. The majority of the earthquakes in the sequence fell near to an approximately linear trend striking northwest. Focal mechanisms of several of the larger events, including the main shock, are all

consistent with right-lateral motion on a northwest-striking structure. Some of the earthquakes occurred later in the sequence seemed to be consistent with a northeast-trending, south-dipping fault (Figure 1). No faults have been identified at the surface that might have accommodated the co-seismic slip. Nevertheless, from a regional perspective, the sequence appeared to contribute to the northwest motion of the Sierra Nevada, as a part of the Pacific-North America plate margin.

The importance of the unusually shallow Mogul sequence for discrimination studies can be seen in Figures 3 and 4. The Mogul mainshock exhibited unusual attenuation properties (Anderson *et al*., 2009). The observed near-field peak accelerations (Figure 3, left plot) were above average for an M_w 5.0 earthquake, up to two standard deviations above the median at station MOGL. The waveforms (Figure 4) showed that these accelerations are not due to isolated spikes, but in fact, reasonably reflected the ground motions. A possible explanation of these high accelerations was the shallow hypocentral depth of the main shock, estimated at a depth of 3.1 km beneath the surface (Ken Smith, pers. comm.). Near-field peak velocities (Figure 3, right plot) were at or above predictions (Campbell and Bozorgnia, 2008). Peak acceleration and peak velocity decreased more rapidly with distance than predicted, to values below the median predictions at most stations in the Reno and Carson City metropolitan areas. One possible explanation for the rapid amplitude decay with distance is that down-going energy was being absorbed near the source in layers of rock that would normally be above an earthquake at a more typical depth. This extreme attenuation would have significant effects on magnitude estimates at local and regional distances. We plan to investigate the degree to which these amplitude anomalies were a general property of the Mogul sequence and the extent of the anomalous attenuation effects on explosion-related discriminants. We anticipate that the spectra of Mogul events will reflect their anomalous depth and near-source attenuation.

The Mogul earthquake results will be compared to relevant measures for nuclear explosions, and other very shallow event results, discussed below.

2) Mining explosions (M_L>2.0) in the Reno-Carson City, NV, area. We are sorting and relocating a mining explosion database including at least 37 re-located quarry blasts in the Reno-Carson City, NV, area. Explosions are not routinely located by the NSL seismic analysts, thus, we are currently conducting a careful re-examination of the records from 1995-2011 for good quality shallow events (M_L > 1.5), to find more explosions within 100 km of the Mogul sequence.

3) Crustal earthquakes (M_L>2.5) within 100 km of Reno, NV. High quality waveforms of crustal earthquakes (M_L>2.5) in the project area will be added to the database. Events from an earthquake sequence that occurred south of Reno (main shock M_L 3.0, 12 km deep, on 11/28/2010, 09:47:38) and events from the 2011 Hawthorne earthquake sequence (main shock M_L 4.6, 15 km depth, on 04/16/2011, 17:45:37) will also be added to the database. The NSL - estimated depth for the Hawthorne earthquakes range from 2 - 17 km.

4) The waveforms from the 1993 Rock Valley sequence (depth < 3 km, m_b≤4.3). We have archived the waveforms from the 1993 Rock Valley sequence (Smith *et al.*, 1996) into an Antelope database. P/Lg ratios have been estimated for this sequence by Walter *et al.*, 1995, and compared to Little Skull Mountain earthquakes and nuclear explosions detonated at the Nevada Test Site, however, supplementary results from these earthquakes would provide useful comparisons to the Mogul sequence. NSL located more than 100 earthquakes ($4.3 \geq m_b \geq 1.1$) on the Nevada Test Site, in Rock Valley, in 1993. These events were unusual in that their hypocenters were very shallow (1-3 km deep), as determined from recordings at portable stations installed near the epicenters, similar to near-field stations in Mogul. Data from the analog Southern Great Basin Seismic Network (SGBSN) and from the digital portable stations for most of these events is available at NSL and will be added to the project database. The largest event in this sequence was M_w 3.7 (m_b 4.3), and eleven events had $M_w \geq 2.5$. Our studies of this sequence will build on work by Mayeda and Walter (1996).

5) Records of the Crandall Canyon mine collapse (0.6 km depth, M_L 3.9), a seismic event which occurred on August 6, 2007, at 08:48:40 UTC, **and of USGS-located events (M_L > 2.5) within 100 km of the mine**.

Our future investigations will start with the second task, which consists of stress drop and radiated energy analysis of the main shock, principal foreshocks and principal aftershocks, and investigations of source scaling of the Mogul sequence. We will estimate source parameters for M_L≥3.5 Mogul events using three related methods. As a first approach, we will model near-field station recordings directly. Initially the model will assume a form of Brune spectral shape with a linear spectral decay associated with kappa. Algorithms to implement this method, based on the approach of Humphrey and Anderson (1992) exist at NSL. The routine is simpler than a moment tensor inversion and provides a magnitude estimate based on a single station. A second approach to estimate stress drop

and radiated energy will be using empirical Green's Functions (EGF's). For small enough events, EGF's can be used as proxies for unknown path effects, thus isolating the remote source. For example, preliminary observations suggest that the source duration of the main shock was about 1.0 seconds, but with the main energy coming in a more compact pulse with duration of about 0.5 seconds. Assuming the S-wave velocity at the source depth of about 2.5 km/s, we expect a fault length of no more than ~2.5 km. If the radius is 1.0 km, combined with one of the estimates of the seismic moment of 3.5 x 10^{23}dyne-cm, and the relationship (Kanamori and Anderson, 1975):

$$M_0 = \frac{16}{7}\Delta\tau_S a_E^3$$

where a_E is the radius and $\Delta\tau_S$ is stress drop, the stress drop would be ~150 bars. Inversion for the slip function using appropriate empirical Green's Functions of known moment will improve the moment estimate, and the source radius estimate. If this high stress drop is confirmed for this shallow earthquake, it may be a case where the stress drop is well constrained and accounts for a large fraction of the lithostatic stress. The stress drop in the main shock will be compared with stress drop in the smaller events. Care will be needed, in analyzing the smaller events, to minimize the tradeoff of stress drop and kappa. We will also evaluate whether the stress drop varies among foreshocks, the mainshock, and aftershocks (Baltay et al., 2010, 2011). A third approach for investigation of stress drop and radiated energy will use measurements of coda envelopes at different frequencies (Mayeda and Walter, 1996; Mayeda et al., 2003, Malagnini et al., 2004). The moment magnitude and seismic stress drop of an event will be determined by fitting the decay rate of *Lg* or *Sn* phase coda via the method of Mayeda et al. (2003). In a densely instrumented region, coda-derived M_w estimates can then be made over a much broader range of earthquake sizes (M_w 2 - 5).

For local - to - regional high-frequency discrimination we will estimate how earthquakes scale with size (Abercrombie et al., 2009). Normally, path attenuation and scattering are convolved with the source terms in regional recordings, making their separation difficult. Near-source recording of the Mogul earthquakes provide an independent means to estimate the source terms and to isolate and separate apparent source scaling in more distant spectra introduced by path effects. We will evaluate scattering contributions to apparent source scaling by exploiting the azimuth coverage of broadband stations. Closely following the methods used by Abercrombie et al. (2009), we will investigate source scaling of Mogul earthquakes for events with $2.0 < M_L < 4.7$. Abercrombie et al, 2009 investigated earthquake sources and scaling from different tectonic settings, comparing direct and coda wave analysis methods that both make use of Empirical Green's Function earthquakes to remove path effects. We plan to use the coda methods, since these authors show that coda and direct wave methods applied to the same datasets provide the same scaling. The Abercrombie et al. (2009), coda wave analysis method uses spectral ratios (as for the direct waves) but relies on the averaging nature of the coda waves to use EGF events that do not meet the strict criteria of similarity required for the direct wave analysis. We will extend this approach by using near-event measurements of the source term. By comparing the apparent source scaling rate of the Mogul events to results in other areas we expect to be able to isolate the depth contribution to apparent source scaling.

For the third task, we will investigate the effect of source depth on *P* and *S* spectra and spectral ratios, signal complexity, and m_b-M_s discrimination. We will test low- to high-frequency spectral-amplitude ratio discriminants on each of the phases *Pn, Pg, Sg, Sn* and *Lg* for the events in the database. Like in Walter et al. (1995), we will assess the dependence on magnitude and the effect of averaging over multiple stations. We will examine regional and teleseismic signal complexity, for array and single station data. The complexity discriminant was proved by Taylor and Anderson (2009) to improve overall discrimination capability in a multivariate framework. Although the complexity discriminant by itself shows marginal performance, Taylor and Anderson indicate that, when complexity discriminants are combined with *mb – Ms,* there is a tendency for explosions, shallow earthquakes and deep earthquakes to form three distinct populations. The complexity factor was defined as the logarithm of the ratio of the average energy (mean square) of the coda in the 5 to 25 second window after the *P*-arrival time and the average signal energy in the 5-second window after the *P*-arrival time. We will evaluate whether the Mogul sequence falls into the category of typically shallow earthquakes, with complex *P*-wave signatures relative to single charge explosions (Taylor and Anderson, 2009).

One of the most established criteria for screening seismic events (Marshall and Basham; 1972; Blandford 1982; Stevens and Day, 1985) is based on a comparison of body-wave magnitude (m_b) and surface wave magnitude (M_S). The null hypothesis is that $m_b > M_s$ for nuclear explosions. The test discriminant is formed from the difference of network averaged surface-wave and body-wave magnitudes. We will compare estimates of m_b for the Mogul main shock and, as possible, for smaller events and other events in the database, using conventional averaging between

the individual station magnitude measurements and the Maximum Likelihood Estimation (Ringdal, 1976). We will use the joint maximum likelihood method, as described by Zaslavsky-Paltiel and Steinberg, (2009) and closely follow their procedures. We will apply to the Mogul sequence and other events in the database the M_s (VMAX) or Variable-period MAXimum amplitude magnitude. M_s (VMAX) is a time-domain technique for determining surface wave magnitudes at variable periods between 8 and 25 s using both regional and teleseismic waves (Russell, 2006; Bonner et al., 2006).

In the fourth task we will attempt to understand the origin and nature of the exceptional near-source attenuation and its effect on magnitude estimates and energy content-related discriminant performance. We will confirm that other principal foreshocks and aftershocks follow the trend of high ground motions (low attenuation) for up-going phases and extreme attenuation of down-going phases seen in Figure 3. This will test whether the extremes seen in Figure 3 are unique to the main shock or are a general property of the source area and shallowness of the seismicity. We will also estimate attenuation effects on *Pn*, *Pg*, and *Lg* amplitudes, spectra, and ratios and we will compare magnitudes including $m_b(P_n)$ to magnitudes based on near-field measurements.

CONCLUSIONS AND RECOMMENDATIONS

We are currently within the first phase of a research program in which we aim to investigate the effectiveness of discrimination algorithms when applied to an unusually shallow (1-4 km deep) sequence of well-documented earthquakes, occurred in 2008 in Mogul, near Reno, Nevada. We are currently building a detailed shallow event database, including the Mogul earthquakes and other relevant earthquake sequences and explosions. Preliminary assessments based on peak ground accelerations and peak velocities show that this unusually shallow earthquake sequence has uncharacteristically high amplitude near-field ground motions and uncharacteristically rapid attenuation with distance, which could affect the magnitude estimates and the discrimination metrics.

In the future we will analyze the stress drop and radiated energy of the Mogul main shock, principal foreshocks, and principal aftershocks, we will investigate the source scaling and we will test the effectiveness of a set of established discrimination methods when applied to the Mogul sequence and other relevant shallow events. We will also attempt to understand the origin and nature of the near-source attenuation and its effect on magnitude estimates and energy content-related discriminant performance.

REFERENCES

Anderson, J. G., Tibuleac, I. M., Anooshehpoor, A., Biasi, G., Smith, K., and D. von Seggern (2009). Exceptional ground motions recorded during the 26 April 2008 Mw 5.0 earthquake in Mogul, Nevada, *Bull. Seismol. Soc. Am.* 99: 3475–3486, doi: 10.1785/0120080352.

Abercrombie, R. E., K. M. Mayeda, William R. Walter, Gisela M. Viegas, and Rengin Gök, (2009). Seismic source scaling and discrimination in diverse tectonic environments, in *Proceedings of the 2009 Monitoring Research Review: Ground-Based Nuclear Explosion Monitoring Technologies*, LA-UR-09-05276, Vol. 1, pp. 419–429.

Baltay, A., G. Prieto, and G. C. Beroza (2010). Radiated seismic energy from coda measurements and no scaling in apparent stress with seismic moment, *J. Geophys. Res.* 115: B08314, doi:10.1029/2009JB006736.

Baltay, A., S. Ide,G. Prieto, and G. Beroza,(2011). Variability in earthquake stress drop and apparent stress, *Geophys. Res. Lett.* 38: L06303, doi:10.1029/2011GL046698.

Bonner, J. L., D. Russell, D. Harkrider, D. Reiter, and R. Herrmann, (2006). Development of a time-domain, variable-period surface wave magnitude measurement procedure for application at regional and teleseismic Distances, Part II: Application and *Ms —mb* Performance. *Bull. Seismol. Soc. Am.* 96*:* 678–696.

Blandford, R. (1982). Seismic event discrimination, *Bull Seismol. Soc. Am* 72: S69–S87.

Campbell, K. W. and Y. Bozorgnia (2008). NGA ground motion model for the geometric mean horizontal component of PGA, PGV, PGD and 5% damped linear elastic response spectra for periods ranging from 0.01 to 10 s, *Earthquake Spectra* 24/1: 139–171.

Fletcher, J., L. Haar, T. Hanks, L. Baker, F. Vernon, J. Berger, and J. Brune (1987). The digital array at Anza, California: processing and initial interpretation of source parameters, *J. Geophys. Res*. 92: 369–382.

Frankel, A., J. Fletcher, F. Vernon, L. Harr, J. Berger, T. Hanks, J.N. and Brune (1986). Rupture characteristics and tomographic source imaging of $M_L \approx 3$ earthquakes near Anza, southern California: *J. Geophys. Res.* 91: 12633–12650.

Kanamori H. and D.L. Anderson (1975). Theoretical basis of some empirical relations in seismology, *Bull. Seismol. Soc. Am*. 65: 1073–1096.

Malagnini, L., K. Mayeda, A. Akinci, and P. Bragato (2004). Estimating absolute site effects, *Bull. Seismol. Soc. Am*. 94/4: 1343–1352.

Marshall, P. D. and P. W. Basham (1972). Discrimination between earthquake and underground nuclear explosion, *Geophys. J. R. Astr. Soc*. 28: 431–458.

Mayeda, K. and W.R. Walter (1996). Moment, energy, stress drop, and source spectra of western U.S. earthquakes, *J. Geophys. Res*. 101: 11195–11208.

Mayeda, K., A. Hofstetter, J. L. O'Boyle, and W. R. Walter (2003). Stable and transportable regional magnitudes based on coda-derived momentrate spectra, *Bull. Seism. Soc. Am.* 93: 224–239.

Prejean S. and W. L. Ellsworth, (2001). Observations of earthquake source parameters at 2 km depth in the Long Valley Caldera, Eastern California, *Bull. Seismol. Soc. Am.* 91/2: 165–177.

Ringdal, F. (1976). Maximum likelihood estimation of seismic magnitude, *Bull. Seismol. Soc. Am.* 66: 789–802.

Russell, D. R. (2006). Development of a time-domain, variable-period surface wave magnitude measurement procedure for application at regional and teleseismic distances, part I: theory, *Bull. Seismol. Soc. Am*. 96/2: 665–677.

Smith, K., von Seggern, D. H., dePolo, D., Anderson, J. G., Biasi, G. P., Anooshehpoor, R. (2008). Seismicity of the 2008 Mogul-Somersett West Reno, Nevada Earthquake Sequence, *Eos Trans. AGU* 89, Fall Meet. Suppl., Abstract S53C-02.

Smith, K., G. Shields, and James N. Brune (2006). A sequence of very shallow earthquakes in the Rock Valley Fault Zone, Southern Nevada Test Site in geologic and geophysical characterization studies of Yucca Mountain, Nevada, Chapter L, 1-11.

Stevens, J. L. and S. M. Day (1985). The physical basis of mb :Ms and variable frequency magnitude methods for earthquake/explosion discrimination, *J. Geophys. Res*. 90: 3009–3020.

Taylor, S. and D. N. Anderson (2009). Rediscovering Signal Complexity as a Teleseismic Discriminant, *Pure and Appl. Geophys.* 166: 325–337.

Walter, W. R, Kevin M. Mayeda, and Howard J. Patton (1995). Phase and spectral ratio discrimination between NTS earthquakes explosions. Part I: empirical observations, *Bull. Seismol. Soc. Am.* 85/4: 1050–1067.

Zaslavsky-Paltiel and David M. Steinberg, (2008). Comparison of methods for estimating station magnitude corrections for improved seismologic monitoring of the Comprehensive Nuclear-Test-Ban Treaty, *Bull. Seismol. Soc. Am.* 98/1:1–17, doi: 10.1785/0120070019.

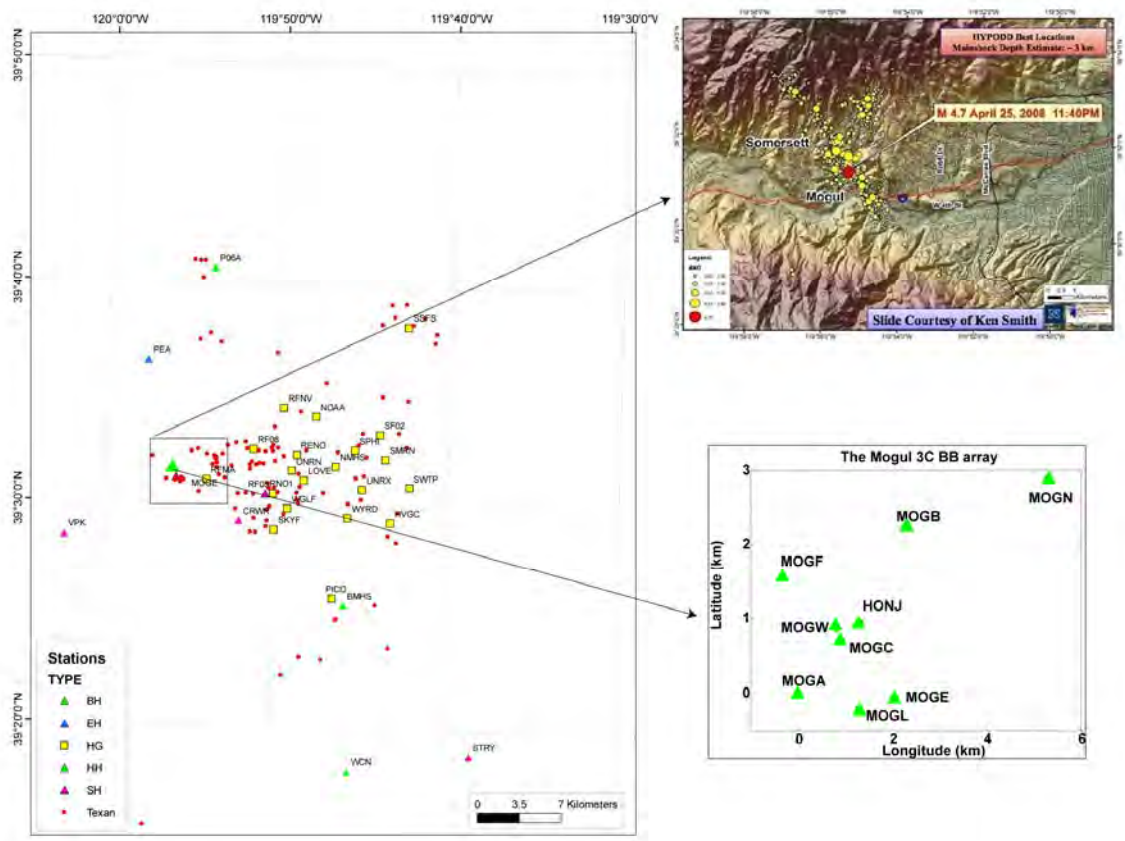

Figure 1. Permanent and temporary stations recording the Mogul sequence. Lower-right inset shows the IRIS Rapid Array Mobilization Program (RAMP) deployment. Stations MOGE, MOGL, MOGW, and HONJ recorded the mainshock and the most energetic fore- and aftershocks. "Texan" digitizers were deployed with high frequency geophones to study basin structure using natural sources, and recorded continuously for only three days at each point. The seismicity of the Mogul sequence is shown in the upper right plot (Smith et al., 2008). Earthquakes shown are from a set relocated with a double-difference algorithm.

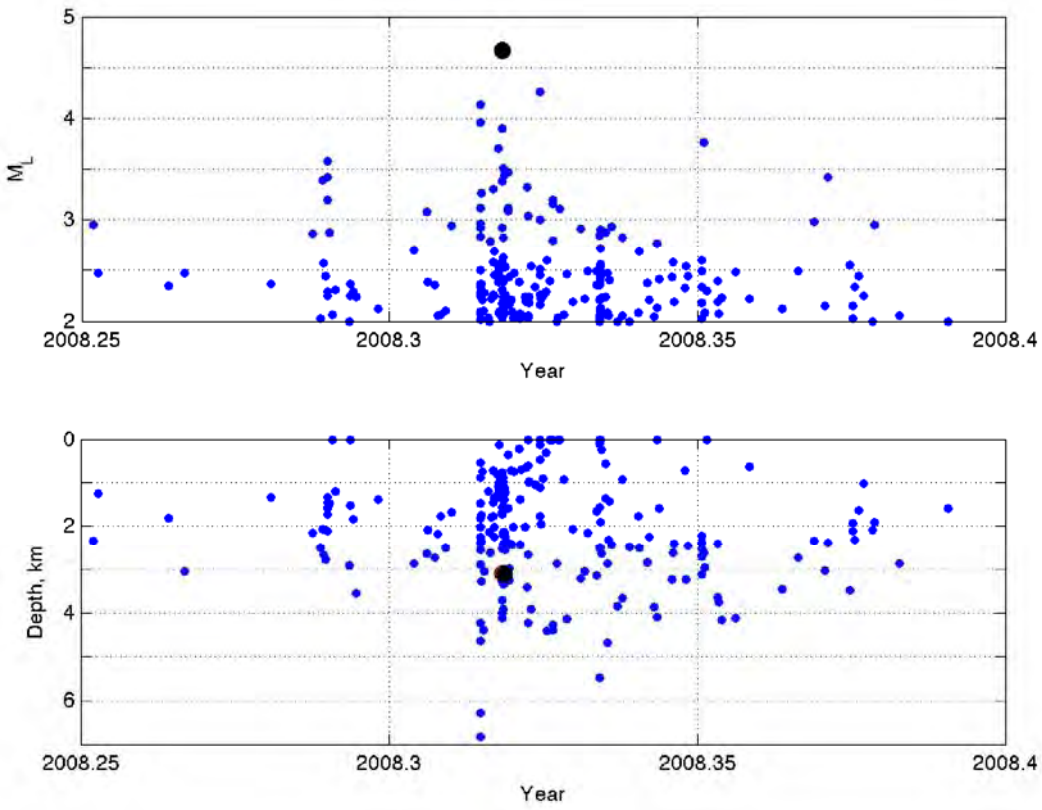

Figure 2. The upper plot shows the local magnitude of the Mogul earthquakes as a function of time. The lower plot shows the preliminary NSL Mogul earthquake depth estimates as a function of time. The main shock is represented as a black dot. The nearest station, MOGE, is at 1.440 km elevation, and the hypocenter of the main event is 3.1 km below MOGE. Although the sequence continued until the end of 2008, only two equal time intervals are represented, including most of the events before and after the main shock.

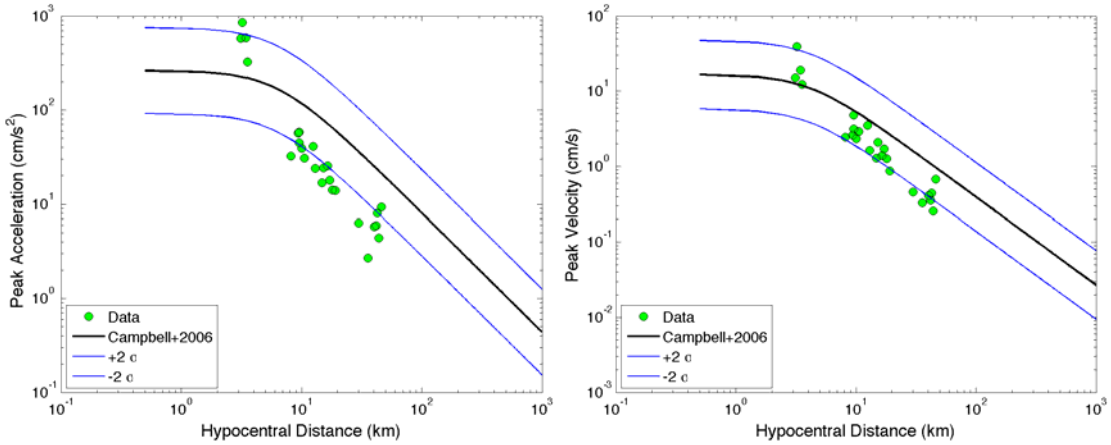

Figure 3. Peak ground acceleration and peak ground velocity for the Mogul main shock from the NSL-operated strong-motion stations. Data points show the geometric mean of the two horizontal components. Peak ground accelerations and peak ground velocities were well above the median expectations (Anderson et al., 2009) in the epicentral area, however, they were below median ground motion predictions (heavy lines, Campbell and Bozorgnia, 2008) at distances of 10 km or more. Thin lines show amplitudes that are within 2σ of the median prediction.

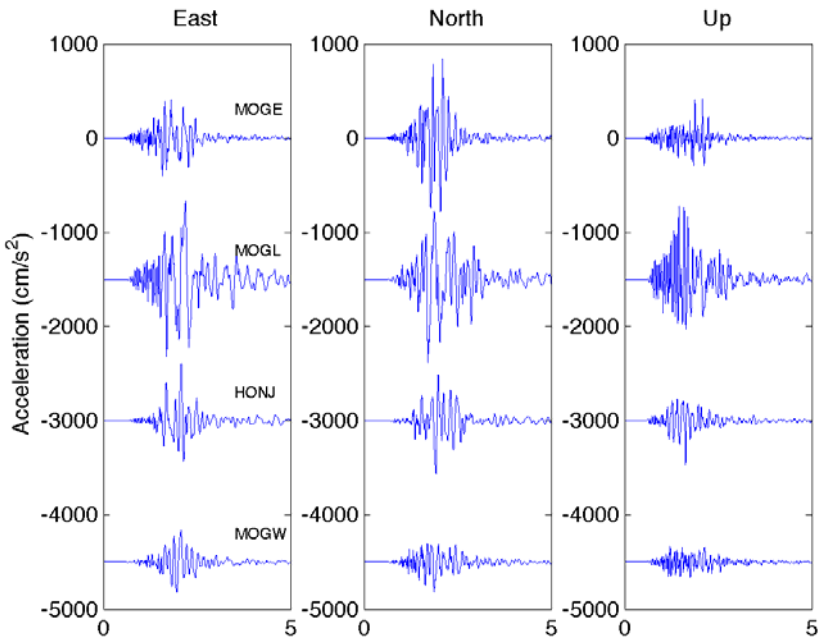

Figure 4. Shows strong motion recordings of the Mogul main shock (Anderson et al., 2009) on the east component (left plot), north component (middle plot) and vertical component (right plot). The plots show accelerations recorded at the four nearest stations MOGE, MOGL, HONJ and MOGW (shown from top to bottom in each plot) during the main shock as a function of time (s). Because the stations are very close to the fault, the *S*-wave begins to arrive from the hypocenter before the end of the *P*-waves from other parts of the fault. The waveforms are typical ground motions, except that they have peak amplitudes that are higher than expected (Figure 3). The records start at the origin time of the earthquake. Except for station MOGE, traces are offset from zero as a plotting convenience.